Biochimica et Biophysica Acta 1862 (2016) 93–104

Contents lists available at ScienceDirect

Biochimica et Biophysica Acta

journal homepage: www.elsevier.com/locate/bbadis

D-ribose-glycation of insulin prevents amyloid aggregation and produces cytotoxic adducts

Clara Iannuzzi [a], Margherita Borriello [a], Vincenzo Carafa [a], Lucia Altucci [a,c], Milena Vitiello [a], Maria Luisa Balestrieri [a], Giulia Ricci [b], Gaetano Irace [a], Ivana Sirangelo [a,*]

[a] Department of Biochemistry, Biophysics and General Pathology, Second University of Naples, Naples, Italy
[b] Department of Experimental Medicine, Second University of Naples, Naples, Italy
[c] Institute of Genetics and Biophysics Adriano Buzzati-Traverso, IGB-CNR, Naples, Italy

ARTICLE INFO

Article history:
Received 19 August 2015
Received in revised form 9 October 2015
Accepted 17 October 2015
Available online 28 October 2015

Keywords:
Insulin glycation
D-ribose
Amyloid aggregation
ROS production
NF-kB
Apoptosis

ABSTRACT

Insulin is a key hormone regulating glucose homeostasis, intimately associated with glycemia and is exposed to glycation by glucose, reducing sugars and other highly reactive carbonyls, particularly in diabetes. Glycation of insulin has been reported to differentially affect protein structure, stability and aggregation depending on the glycating agent and experimental conditions. Under reducing conditions glycation produces higher insulin oligomerization thus accelerating amyloid formation whereas, in non-reducing conditions, glycation inhibits amyloid formation. To better detail the effect of glycation on insulin malfunction and toxicity, we investigated the effect of another glycating agent, the D-ribose. Recently, ribosylation has received great interest due to its role in protein glycation and its consequential effects such as protein aggregation, oxidative stress and cell death. Moreover, unusual high concentration of D-ribose has been detected in the urine of type II diabetics.
Our results show that, using ribose, as glycating agent, the insulin conformation is preserved and does not evolve in amyloid aggregates because of the block of the α-helix to β-sheet transition, which initiates the aggregation process, maintaining the protein in a soluble state. At the same time, ribose-glycated insulin strongly affects the cell viability, starting a death pathway consisting in the activation of caspases 9 and 3/7, intracellular ROS production and activation of the transcription factor NF-kB.

1. Introduction

Insulin is a key hormone regulating glucose homeostasis and a widely used drug for treatment of diabetes. Insulin is composed of two peptide chains, the A chain and the B chain, linked by two disulfide bonds. The A chain consists of 21 amino acids organized in two α-helices connected by a loop and contains an intra-molecular disulfide. The B chain consists of 30 amino acids organized in an α-helix in the central region of the molecule flanked by two turns and flexible regions in both termini [1].

Insulin is stored in the pancreas as inactive zinc hexamer; when released into the blood serum, the hexameric form dissociates into a dimer and then subsequently into a monomer, which is the physiologically active form [2]. However, the insulin monomer is less stable than the hexamer and tends to aggregate forming amyloid aggregates [3,4]. Insulin is able to form amyloid-like fibrils in the site of medication injections of insulin-dependent diabetic patients causing a pathological condition, called insulin injection amyloidosis [5–9]. A variety of human diseases including neurodegenerative diseases, are related to the formation of protein aggregates, named amyloid fibrils [4,10]. Amyloid fibrils are characterized by a common structural motif, the cross-β-structure in which individual strands in the β-sheets run perpendicular to the long axis of the fibril. Insulin has been widely used as a model protein for the study of the amyloid formation. In fact, under specific conditions, i.e., high temperature and low pH, it is very prone to form amyloid fibrils [11–12]. At pH 2, insulin forms soluble assemblies in equilibrium with monomers and smaller oligomers [13]. At high temperatures, these species further assemble into larger irreversible aggregates and eventually in amyloid fibrils. The α to β- transition seems to occur only upon fibril assembly, while the initial aggregates retain their predominantly helical structure [14–15].

Insulin is associated with glycemia and can be susceptible to glycation by glucose and other highly reactive carbonyls especially in diabetic conditions [16]. Glycated insulin is unable to regulate glucose homeostasis in vivo and to stimulate glucose transport and adipose tissue lipogenesis [17–19]. Protein glycation is a non-enzymatic, irreversible modification resulting from a chemical reaction of reducing sugars with primary amino groups (N-terminal, and arginine and lysine side chains). Spontaneous glycation includes the reversible formation of a Schiff base which is transformed into a product of Amadori, which can

* Corresponding author at: Department of Biochemistry, Biophysics and General Pathology, Second University of Naples, via L. De Crecchio 7, 80138 Naples, Italy.
E-mail address: ivana.sirangelo@unina2.it (I. Sirangelo).

http://dx.doi.org/10.1016/j.bbadis.2015.10.021
0925-4439/

further rearrange to give advanced glycation end products (AGEs) [20–21]. Accumulation of AGEs has been suggested to be a main factor responsible for diabetes-associated complications, such as retinopathy, nephropathy, atherosclerosis [22–28]. In addition, AGEs have been recently linked to amyloid based neurodegenerative diseases [29–30]. Different proteins associated with these diseases, such as ß-amyloid, tau, prions and transthyretin, have been found to be glycated in patients [31–34], suggesting a possible role of glycation in amyloid pathogenesis. Moreover, glycation of proteins has been reported to destabilize the native state and stimulate protein aggregation as well as amyloid deposition [35–43]. Other studies suggest that glycation in proteins does not promote modifications in the secondary structure but rather stabilizes the native conformation inhibiting aggregation [44–47]. However, the mechanism by which glycation modulate protein aggregation is still poorly understood. According to the type of reacting sugar, the target protein undergoes specific modifications that may either increase or suppress protein fibrillation.

In physiological conditions, kinetics of AGE formation is quite slow, while in diabetes their formation dramatically increases due to the chronically high concentration of blood sugar [26,48-51]. AGEs damage cells by affecting the structure and function of proteins as well as interacting with specific cellular receptors, between them the best characterized is the one for AGE (RAGE). High concentrations of AGEs, as observed in diabetes, led to an increased expression of the receptor in cells of the blood vessel wall, including endothelium and vascular smooth muscle cells, and promote invasion of circulating immune cells [27,52]. Activation of RAGE is tightly connected to the sustainment of the inflammatory response, resulting in chronic inflammation, as observed in diabetes. The interaction of AGEs with RAGE triggers a range of cellular responses, including transcription factor activation and changes in gene expression. Binding of ligands to RAGE results in the activation of NADPH-oxidases that leads to an increased production of reactive oxygen species (ROS). One major downstream target of RAGE is the pro-inflammatory NF-kB-pathway, which in turn leads to elevated RAGE expression and perpetuation of the cellular inflammatory state [53-55].

Glycation of insulin has been reported to differentially affect protein structure, stability and aggregation depending by glycating agent and/or environmental conditions. In vitro experiments have shown that insulin can be glycated by glucose able to react with Lys29 in the C-terminal region of chain B and with N-terminus of chains A and B [56, 57]. Glucose induces the formation of glycated insulin adducts having different structural features depending on the experimental conditions used. In particular, glycation in reducing conditions is able to induce insulin oligomerization thus accelerating amyloid formation. On the contrary, glycation in non-reducing conditions strongly inhibits amyloid formation in a way proportional to the glycation extent [58]. The effects of glycation by methylglyoxal on the structure and fibril-forming properties of insulin have been also investigated [46]. Human insulin can be glycated also by methylglyoxal able to react with a single site, i.e., Arg22 of the B-chain. This modification promotes the formation of native-like aggregates and reduces the ability of human insulin to form fibrils by impairing the formation of the seeding nuclei. These aggregates are small, soluble, non-fibrillar and retain a native-like structure [46].

In this paper, to clarify the effect of glycation on insulin malfunction and toxicity, we report the effect of another glycating agent, the D-ribose, in comparison with MG, on the structure and aggregation propensity. Moreover, we analyze the effect of ribosylated insulin on cell viability. Recently, an increasing interest has been focused on protein ribosylation due to its role in protein glycation and its consequent effects such as protein aggregation and ROS production [59]. Moreover, abnormally high concentration of D-ribose has been recently found in the urine of type II diabetic patients [60]. Our results show that both glycating agents used, by blocking the α-helix to β-sheet transition, preserve the insulin conformation unable to evolve in amyloid aggregates. Thus, AGE formation inhibits amyloid aggregation in human insulin but strongly affects the cell viability. Molecular bases of cell toxicity induced by AGEs upon ribosylation of human insulin have been also investigated.

2. Materials and methods

2.1. Materials

Thioflavin T (ThT), 3-(4,5-dimethylthiazol-2-yl)-2,5-diphenyl-tetrazolium bromide (MTT), D-ribose, 2′,7′-dichlorofluorescin diacetate, N-acetylcysteine (NAC), human insulin, methylglyoxal, (Sigma-Aldrich Co., St. Louis, MO). Uranil acetate replacement stain (Electron Microscopy Sciences, Hatfield, PA). Primary antibodies: rabbit anti NF-kB p65 (C22B4 Cell Signaling Technology, Danvers, MA), rabbit anti α-tubulin (ab4074, Abcam), rabbit anti HistoneH1 (ab61177, Abcam), mouse anti Vimentin (Sigma-Aldrich Co., St. Louis, MO). Secondary antibodies: Alexa Fluor 488 and Alexa Fluor 633 (Life Technologies Italia, Monza, Italy). All other chemicals were of analytical grade. Methylglyoxal was further purified by distillation under low pressure and its concentration was determined spectrophotometrically using $\varepsilon_{284} = 12.3\ M^{-1}\ cm^{-1}$ [61].

2.2. Insulin preparation and glycation

Human insulin was dissolved in ultra-pure milliQ water to a final concentration of 4 mg/mL, acidified to a pH of 4 in order to obtain monomeric insulin and protein concentration determined by absorbance ($\varepsilon_{275} = 4560\ M^{-1}\ cm^{-1}$). Finally, insulin was neutralized to pH 7.0 and kept in phosphate buffer 50 mM, pH 7.0.

Glycated insulin was prepared by mixing human insulin at a final concentration of 2 mg/mL in 0.5 M D-ribose or 5 mM methylglyoxal in 50 mM NaH_2PO_4 buffer, pH 7.0, passed through a 0.22 μm filter and incubated at 37 °C in sterile conditions. Human insulin in buffer without glycating agent was used as protein control. A control sample having the same amount of glycating agent but with buffer was incubated under identical conditions.

For aggregation studies, protein samples were incubated at 37 °C under vigorous stirring with teflon balls, 1/8″ diameter (Polysciences, Inc.). Aliquots were collected in sterile conditions and immediately analyzed.

2.3. Fluorescence measurements

Fluorescence measurements were performed on a Perkin Elmer Life Sciences LS 55 spectrofluorimeter. To assess the intrinsic fluorescence of AGEs (λ_{ex} 320 nm/λ_{em} 410 nm), glycated insulin at a final concentration of 8 μM was monitored at different incubation times with the glycating agent. The fluorescence intensity was corrected by subtracting the emission intensity of D-ribose/methylglyoxal solutions at different incubation times. Tyrosine emission fluorescence spectra were recorded between 280 and 450 nm using a λ_{ex} of 275 nm. ThT fluorescence (λ_{ex} 450 nm/λ_{em} 482 nm) was monitored at different time intervals after addition of ThT to protein samples. Working concentrations were 8 μM for protein samples and 25 μM for ThT. The ThT fluorescence was corrected by subtracting the emission intensity of glycated samples before the addition of ThT.

2.4. Circular dichroism (CD)measurements

CD spectra were recorded at 25 °C on a JascoJ-715 spectropolarimeter using thermostated quartz cells of 0.1 cm. Spectral acquisition was taken at 0.2 nm intervals with a 4 s integration time and a bandwidth of 1.0 nm. An average of three scans was obtained for all spectra. Photomultiplier absorbance did not exceed 600 V in the spectral region analyzed. All measurements were performed under nitrogen flow and spectra were recorded after diluting six times the stock solution (final protein concentration 0.3 mg/mL). Data were corrected for buffer

contributions using the software provided by the manufacturer (System Software version 1.00) and transformed in mean residue ellipticity before analysis. Protein secondary structure estimation was performed using CDPro software, which contains three software packages, i.e., CDSSTR, CONTIN/LL, and SELCON3 [62].

2.5. Gel electrophoresis (PAGE)

The glycation-induced oligomerization was monitored by the protein mobility shift on both native-PAGE and SDS-PAGE (18%) using Bio-Rad (USA) electrophoresis equipment. Ten micrograms of protein sample was loaded and the protein bands were stained with Coomassie Brilliant Blue.

2.6. Immunoblotting

Proteins were separated by 10% SDS-PAGE under reducing conditions, and blotted onto a polyvinylidene difluoride membrane in transfer buffer (25 mM Tris, 192 mM glycine, 20% methanol, 0.1% SDS). The blots were then probed with primary antibodies, followed by the corresponding horseradish peroxidase (HRP)-conjugated secondary antibodies. Immunoreactivity was detected by the ECL reaction (RPN2109, GE Healthcare) and quantified using the ChemiDoc MP Imager Software (Biorad).

2.7. Transmission electronic microscopy (TEM)

Aliquots of protein samples (3 μL) were placed on the copper grid and allowed to dry. After 5–6 min uranil acetate replacement stain 1× (3 μL) was loaded on the grid and air dried. Images were acquired using a Libra 120 (Zeiss) Transmission Electron Microscope equipped with Wide-angle Dual Speed CCD-Camera sharp:eye 2 K (4Mpx.).

2.8. Cell cultures and treatments

NIH-3T3 mouse embryonic fibroblasts (ATCC# CCL-92) were cultured in Dulbecco's modified eagle's medium (DMEM)-high glucose supplemented with 10% bovine calf serum, 3.0 mM glutamine, 50 units/mL penicillin and 50 mg/mL streptomycin in a 5.0% CO_2 humidified environment at 37 °C. CPAE endothelial cells (ECs) (ATCC# CCL-209) were cultured in Minimun Essential Medium (MEM) supplemented with 10% fetal bovine calf serum (USA Origin), 2.0 mM glutamine, 100 units/mL penicillin and 100 mg/mL streptomycin in a 5.0% CO_2 humidified environment at 37 °C. For all experiments, cells in culture medium without protein and in the presence of non-glycated insulin served as control. Before incubation with cells, human insulin glycated in the presence of 0.5 M D-ribose for 8 days was subjected to dialysis in sterile conditions to remove the free glycating agent.

2.9. Cell viability assay

Cell viability was assessed as the inhibition of the ability of cells to reduce the metabolic dye 3-[4,5-dimethylthiazol-2-yl]-2,5-diphenyltetrazolium bromide (MTT) to a blue formazan product [63,64]. NIH-3T3 cells were plated at a density of 100,000 cells/well on 12-well plates in 1 mL of medium. EC were seeded in 96-well at a density of 4000 cells/well. After indicated times of incubation with protein samples, cells were rinsed with phosphate buffer solution (PBS). A stock solution of MTT (5 mg/mL in PBS) was diluted ten times in cell medium and incubated with cells for 3 h at 37 °C. After removing the medium, cells were treated with isopropyl alcohol, 0.1 M HCl for 20 min. Levels of reduced MTT were assayed by measuring the difference in absorbance at 570 and 690 nm. Data are expressed as average percentage reduction of MTT with respect to the control ± S.D. Data are an average from five independent experiments carried out in triplicate.

2.10. Detection of intracellular ROS

Intracellular ROS were detected by means of an oxidation-sensitive fluorescent probe 2′,7′-dichlorofluorescin diacetate (DCFH-DA). ECs were grown in a six-well plates, pre-incubated with DCFH-DA for 30 min and then incubated with protein samples for 12, 24, 48, and 72 h. Control experiments were performed using untreated cells and cells exposed to a 0.001 M H_2O_2. Experiments in the presence of NAC were performed on cells pre-treated with 20 mM NAC for 1 h. After incubation, cells were washed twice with PBS buffer and then lysed with Tris–HCl 0.5 M, pH 7.6, 1% SDS. The non-fluorescent DCFH-DA is converted, by oxidation, to the fluorescent molecule 2′,7′-dichlorofluorescein (DCF). DCF fluorescence intensity was quantified on a Perkin Elmer Life Sciences LS 55 spectrofluorimeter using an excitation wavelength of 488 nm and an emission wavelength of 530 nm. Data are expressed as average ± S.D. from five independent experiments carried out in triplicate.

2.11. Cell-cycle analysis

After 12, 24, 48 and 72 h of incubation with protein samples (30 μM), 2.5×10^5 cells were collected and resuspended in 500 μL of hypotonic buffer (0.1% Triton X-100, 0.1% sodium citrate, 50 μg/mL iodide propidium, RNAse A). Cells were incubated in the dark for 30 min and samples were acquired on a FACS-Calibur flow cytometer using the Cell Quest software (Becton Dickinson) and ModFitLT version 3 software (Verity) as previously reported [65,66].

2.12. FACS analysis of apoptosis and caspase assay

Apoptosis was measured by evaluation of the pre-G1 content using ModFitLT version 3 software (Verity). Caspase activity was detected within living cells using B-BRIDGE Kits supplied with cell-permeable fluorescent substrates, following the manufacturer's suggestions. The fluorescent substrates used were FAM-DEVD-FMK for caspase-3/7; FAM-LETD-FMK for caspase 8; SR-LEHD-FMK for caspase 9. After 48 and 72 h of incubation with protein samples, cells were collected, washed twice in cold PBS and incubated for 1 h on ice with the corresponding substrates. Cells were analyzed using Cell Quest software applied to a FACS-Calibur (BD). Experiments were performed in biological duplicates and values expressed in mean ± SD from five independent experiments.

2.13. Confocal laser-scanning microscopy

Confocal microscope analysis was performed as described [67]. Briefly, cells were fixed with 3% paraformaldehyde and permeabilized with 0.1% Triton X-100 before incubation with specific antibodies against NF-kB (1:100, rabbit) and Vimentin (1:1.000, mouse). Secondary antibodies were Alexa Fluor 488 (1:1000) or Alexa Fluor 633 (1:1000). Microscopy analyses were performed using Zeiss LSM 700 confocal microscope equipped with a plan-apochromat X 63 (NA 1.4) oil immersion objective.

2.14. Cellular nuclear extraction

Control and treated cells (1×10^6 cells) were pelleted by centrifugation, resuspended in lysis buffer (10 mM HEPES pH 7.5, 10 mM KCl, 0.1 mM EDTA, 1 mM dithiothreitol, 0.5% Nonidet-40 and 0.5 mM PMSF along with the protease inhibitor cocktail) and allowed to swell on ice for 15–20 min. Tubes were vortexed to disrupt cell membranes and then centrifuged at 12,000 *g* at 4 °C for 10 min. The supernatant was taken as cytoplasmic extract.

The pelleted nuclei were washed thrice with the cell lysis buffer and resuspended in the nuclear extraction buffer (20 mM HEPES (pH 7.5), 400 mM NaCl, 1 mM EDTA, 1 mM DTT, 1 mM PMSF with protease

inhibitor cocktail) and incubated in ice for 30 min. Nuclear extract was collected by centrifugation at 12,000 *g* for 15 min at 4 °C. Protein concentration of the nuclear and cytoplasmic extract was estimated using Bradford's reagent (BioRad, USA). Cytoplasmic contamination of the nuclear fraction was tested by checking tubulin through western-blot analysis.

2.15. Statistical analysis

For statistical analysis, we used a two-tailed Student's t test with unequal variance at a significance level of 5% unless otherwise indicated.

3. Results

3.1. Effect of glycation on human insulin

Glycation of a protein results in the appearance of a new fluorescence derivative centered at 410 nm ($\lambda_{ex} = 320$ nm) that is widely used to monitor the AGE formation [68]. For this reason, insulin samples were incubated at 37 °C in the presence of D-ribose and changes in its fluorescence intensity were monitored at different time intervals (days). The results were compared to those obtained incubating insulin with methylglyoxal. Fig. 1 shows the time course of the emission intensity at 410 nm of insulin incubated with 0.5 M D-ribose and 5 mM methylglyoxal. The emission intensity of glycated protein increased markedly with incubation time. Methylglyoxal was shown to be much more effective than D-ribose as glycating agent. Indeed, it was able to induce insulin glycation in a shorter time, i.e., glycation is completed in about 4 days whereas D-ribose requires at least 7 days. Human insulin alone, used as a negative control, showed no fluorescence at 410 nm.

Also, we analyzed the glycation induced modification of intrinsic fluorescence of insulin. This protein contains only tyrosyl residues as fluorescence emitter and its spectrum is characterized by the typical tyrosyl emission centered at 305 nm. The emission spectra of human insulin incubated in the absence and in the presence of D-ribose and methylglyoxal for 8 days are shown in Fig. 2A. A decrease of fluorescence intensity of about 20% was detected in the sample glycated with D-ribose in comparison with the non-glycated one, whereas a much stronger reduction of fluorescence intensity (about 45%) was detected in the sample glycated with methylglyoxal. Intensity variation and/or maximum shift of fluorescence emission could be produced by structural changes upon glycation as reported for other glycated proteins [40,59]. However, tyrosine fluorescence is not very sensitive

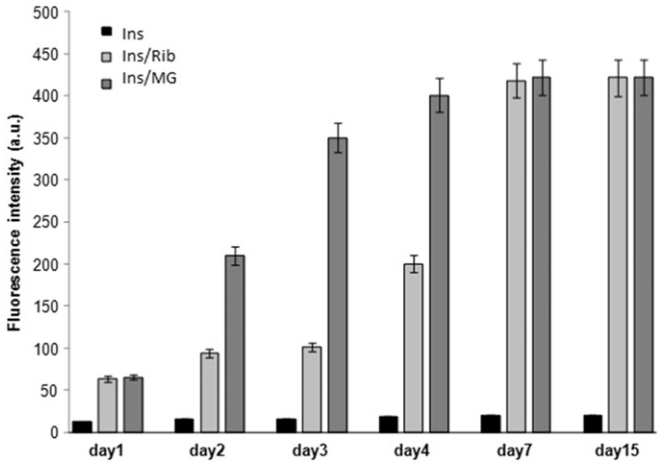

Fig. 1. Glycation kinetics of human insulin. Protein glycation was monitored by fluorescence spectroscopy. Insulin was incubated in the absence (black) and in the presence of 0.5 M D-ribose (light gray) and 5 mM methylglyoxal (dark gray) and samples were analyzed by fluorescence at different time points. Protein concentration was 8 μM, other experimental details are described in the Materials and methods section.

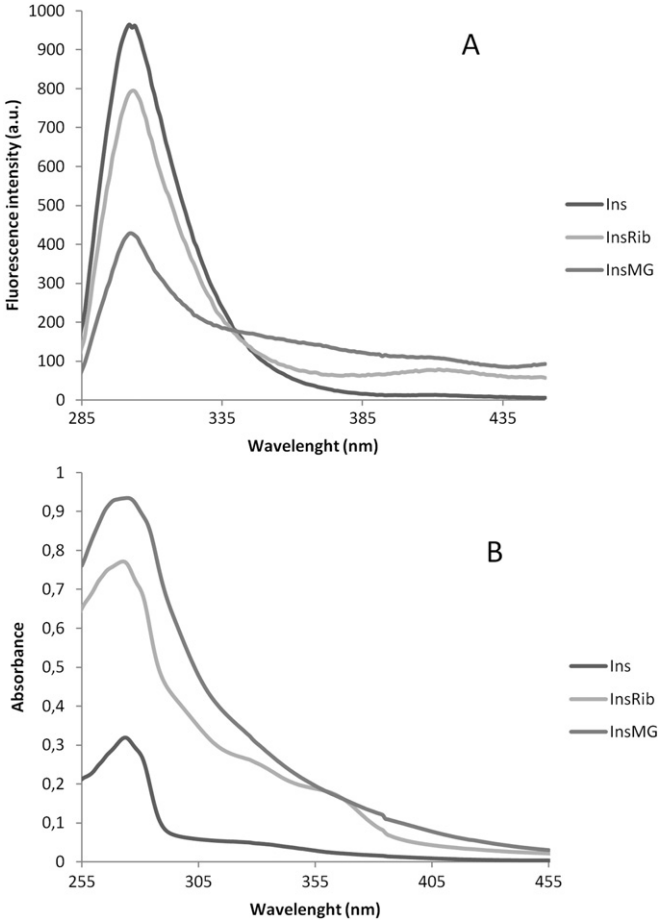

Fig. 2. Effect of glycation on the spectroscopic properties of human insulin. Tyrosine emission fluorescence (panel A) and absorption (panel B) spectra of human insulin incubated in the absence (black) and in the presence of D-ribose (light gray) and methylglyoxal (dark gray) for 8 days. Protein concentration was 8 μM (A) and 40 μM (B). The emission spectrum was recorded upon excitation at 275 nm.

to conformational changes, no shifts in emission maximum being generally detected. Reduction of emission intensity could be due to quenching effect produced by neighboring glycated groups. The appearance of a fluorescence tail centered at 410 nm suggests that an energy transfer occurs between tyrosyl residues and the glycated group. This is further confirmed by inspection of the absorption spectrum recorded upon glycation (Fig. 2B). In fact, the glycated insulin shows an absorption contribution due to AGE formation at wavelength longer than 300 nm, where tyrosyl residues emit. A similar effect has been detected for other proteins [69]. The observation that the extent of quenching is largely different for the two AGE modified insulin adducts formed with D-ribose and methylglyoxal suggests that glycating agents react with different amino groups. A study from Oliveira and coworkers identified ArgB22 as the only glycated residue in insulin in the presence of methylglyoxal [46]. Therefore, we can hypothesize that glycation of ArgB22 induced by methylglyoxal is responsible of the fluorescence quenching both of TyrA19 and TyrB16 that are very close to the ArgB22 in the three dimensional structure of native insulin. Similarly, glycation of Lys29 in the C-terminal region of chain B and on N-terminus of chain A [57] may quench the emission of Tyr B26.

In order to follow changes in secondary structure induced by glycation in human insulin we monitored the dichroic activity in the far-UV region (far-UV CD). After incubation of insulin at 37 °C in the presence and in the absence of 0.5 M D-ribose and 5 mM methylglyoxal, samples were analyzed by CD spectroscopy at different time points. As expected, no difference in the CD activity was detected for the protein without glycating agent at different incubation times (data not

shown). Spectra of human insulin recorded at different times of incubation with D-ribose and methylglyoxal are shown in Fig. 3A and B, respectively. All spectra exhibited two minima at 208 and 222 nm and a positive band below 200 nm typical of a α-helical conformation. No light scattering was detected, indicative of absence of protein aggregation. Although CD spectra of glycated insulin do not exhibit strong shape variation compared to the non-glycated protein, the reduction in the dichroic activity at 222 and 197 nm observed as glycation proceeds is indicative of loss of α-helical structure. Deconvolution analysis of the CD spectra confirmed the loss of α-helical structure upon glycation and a corresponding increase of unordered fraction. In Table 1 is reported the secondary structure content at different glycation times. There is a strong correspondence between the estimated content of secondary structure and the results reported in Fig. 1 clearly indicating that the reduction in the helical content is directly related to glycation extent.

3.2. Ribosylation and insulin oligomerization

Glycation has been indicated as a contributory factor in the formation of high molecular weight protein species which originate from inter molecular cross-links among AGE adducts. [47,58,70,71]. In order to monitor the increase in the apparent molecular weight of glycated adducts, ribosylation of human insulin was evaluated by mobility shift electrophoresis. Both native PAGE and SDS-PAGE were used to analyze

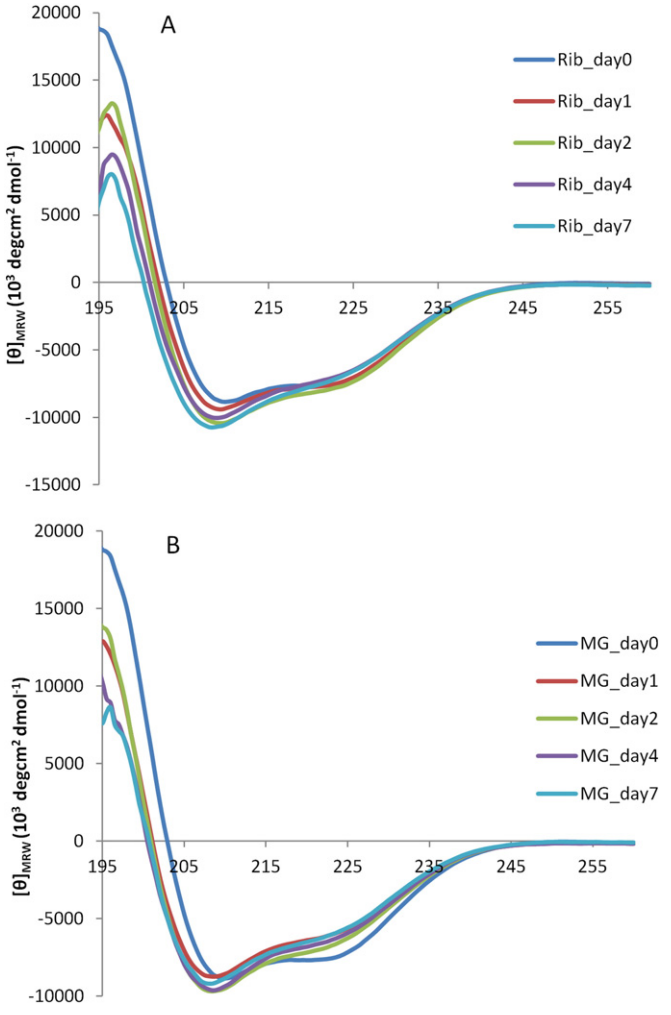

Fig. 3. Effect of glycation on the secondary structure of human insulin. Time dependence of the far-UV CD activity of the human insulin at pH 7.0 in the presence of 0.5 M D-ribose (panel A) and 5 mM methylglyoxal (panel B). Spectra were recorded at indicated times and protein concentration was 0.3 mg/mL.

Table 1
Secondary structure content of human insulin in the absence and in the presence of D-ribose and methylglyoxal at different incubation times.

	Ins	Ins/MG				Ins/Rib			
		Day1	Day2	Day4	Day7	Day1	Day2	Day4	Day7
α-helix	0.41	0.32	0.26	0.21	0.21	0.40	0.38	0.35	0.31
β-strand	0.09	0.13	0.15	0.16	0.16	0.09	0.10	0.12	0.12
Turn	0.20	0.21	0.21	0.22	0.22	0.20	0.20	0.21	0.21
Unordered	0.30	0.34	0.38	0.40	0.41	0.31	0.32	0.32	0.36

Analysis was performed as described in the Materials and methods section and results are expressed as percentage.

samples of insulin at different incubation times (3 and 21 days) in the absence and in the presence of 0.5 M D-ribose (Fig. 4). In the SDS-PAGE, the samples incubated with D-ribose did not show bands at high molecular weight both in the early stage of glycation and after 21 days of incubation, thus indicating that covalent crosslinks are not formed upon glycation (Fig. 4A). This was further confirmed by native PAGE (Fig. 4B), which shows the presence of a single band both for glycated and not glycated insulin. The difference observed in the migration pattern may be ascribed to a modification of the charge/mass ratio produced by glycation of amino groups. Thus, the glycated insulin adduct exhibits a low propensity for oligomerization. When ribosylated insulin was analyzed by SDS-PAGE under non-reducing condition (Fig. 4C), only additional faint bands at low molecular weight were observed, roughly corresponding to insulin dimer and trimer. Being detected only under non reducing conditions, these low molecular weight species cannot be ascribed to cross-linked AGEs adducts but to non native disulfide bonds. Similar results have been reported for insulin glycated with glucose in non reducing condition [58].

3.3. Ribosylation inhibits amyloid fibrils formation in insulin

Amyloid fibrils formation consists of a series of stages including aggregation of soluble oligomers as result of non specific interactions, formation of protofibrillar structures and their assembly into mature fibrils [14,72,73]. Insulin amyloid formation, like other amyloidogenic proteins, occurs through a nucleation and elongation process. Insulin prefibrillar aggregates (oligomers and protofibrils) have a low content of beta sheet in comparison with mature amyloid fibrils, and act as a nucleation agent to form mature fibrils [74]. It has been shown that the oligomeric intermediates are the most toxic species compared to the mature fibrils [71-77]. Human insulin is able to form amyloid aggregates both in denaturing conditions (i.e. pH 2, 60 °C) and in native conditions upon perturbation (stirring). To investigate the effect of ribosylation on the aggregation process of the human insulin, we tested the ability of glycated insulin to form amyloid aggregates in native conditions upon stirring. To this aim, human insulin after glycation with D-ribose for 8 days was incubated at 37 °C with stirring and samples were analyzed at different incubation times by ThT fluorescence (Fig. 5A). The results were compared to those obtained incubating insulin with 5 mM methylglyoxal. ThT fluorescence is a widely used method for detecting amyloid formation as ThT specifically binds amyloid structures exhibiting a strong fluorescence increase [78]. As expected, the non-glycated insulin is able to bind ThT in few hours, thus indicating the formation of amyloid species in a short time upon stirring. On the contrary, no ThT fluorescence increase was detected for samples glycated with both D-ribose and methylglyoxal upon stirring. The fluorescence intensity detected was comparable to that recorded before ThT addition to the same sample. ThT fluorescence was monitored for one month without detecting any fluorescence increase. These results suggest that glycation with both D-ribose and methylglyoxal strongly inhibits amyloid aggregation in insulin. Similar results were observed with methylglyoxal in a previous study that characterized methylglyoxal modification of insulin [46].

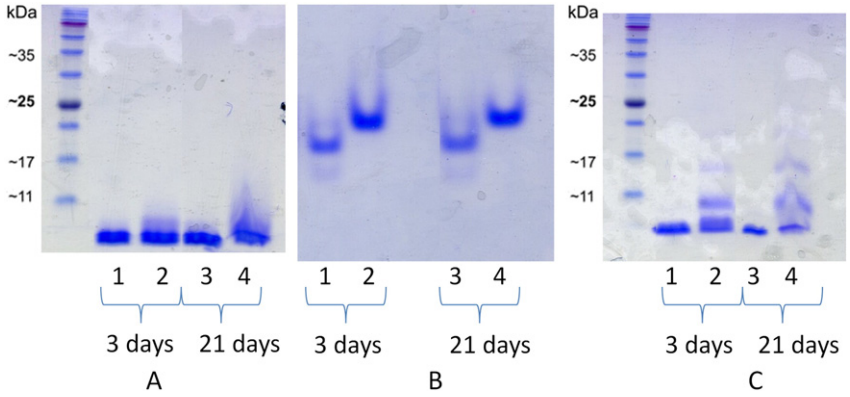

Fig. 4. Effect of glycation on the oligomerization of human insulin. Electrophoresis analysis of human insulin incubated in the absence and in the presence of D-ribose for 3 and 21 days at 37 °C. A, B and C represent the reducing SDS gel, native gel, and non-reducing SDS gel, respectively. Lanes 1 and 3 refer to non glycated insulin, lanes 2 and 4 to glycated insulin. Other experimental details are described in the Materials and methods section.

Samples incubated at 37 °C with stirring for 24 h were also analyzed by far-UV CD spectroscopy (Fig. 5B). The CD spectrum of non-glycated sample strongly differs from that recorded for the ribosylated insulin. In particular, the former showed a very reduced dichroic activity with a concomitant morphology change typical of the α-β transition occurring upon fibril formation. On the contrary, ribosylated insulin showed a spectrum comparable to the one recorded before stirring and reported in Fig. 2. These results indicate that glycation stabilizes the formation of soluble species blocking the α-helix to β-sheet transition characteristic of amyloid fibril formation.

Moreover, we evaluated the viability of cells exposed to non-glycated insulin and ribose-glycated insulin after 24 h of stirring at 37 °C, i.e., under aggregation condition in which the aggregate forms of insulin are not cytotoxic (Fig. 5C). As expected, no toxicity was detected

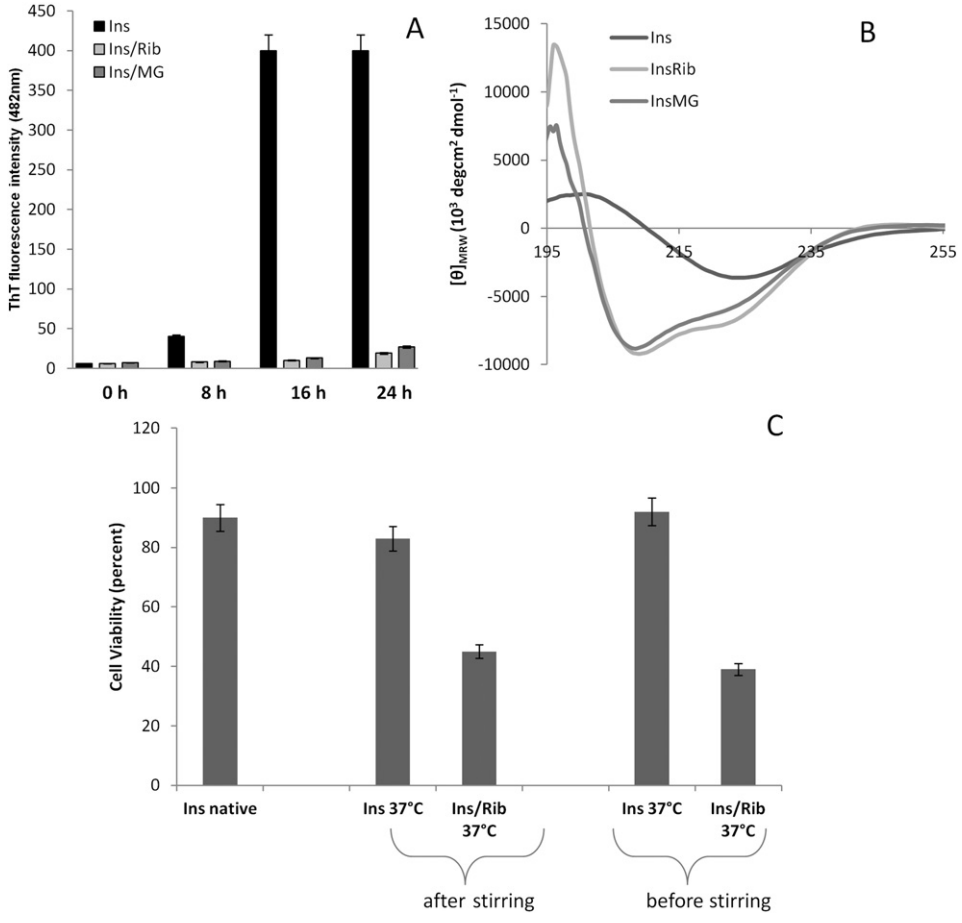

Fig. 5. Effect of glycation on the amyloid aggregation of human insulin. Human insulin incubated in the absence and in the presence of 0.5 M D-ribose and 5 mM methylglyoxal for 8 days was incubated with stirring at 37 °C. Samples were analyzed at the indicated incubation times by ThT fluorescence (panel A), and after 24 h by far-UV CD spectroscopy (panel B). ThT emission was recorded at 482 nm upon excitation at 450 nm; working concentrations were: (A) 8 μM for protein samples and 25 μM for ThT; (B) 0.3 mg/mL. Samples of insulin (40 μM), incubated with stirring at 37 °C for 24 h (after stirring) and before incubation with stirring (before stirring), were exposed to NIH-3 T3 cells for 24 h and cell viability was evaluated by MTT assay (panel C). Data are expressed as average percentage of MTT reduction ± SD relative to control cells from triplicate wells from 5 separate experiments ($p < 0.01$). Cells treated with fresh insulin was also tested. Other experimental conditions are described in the Materials and methods section.

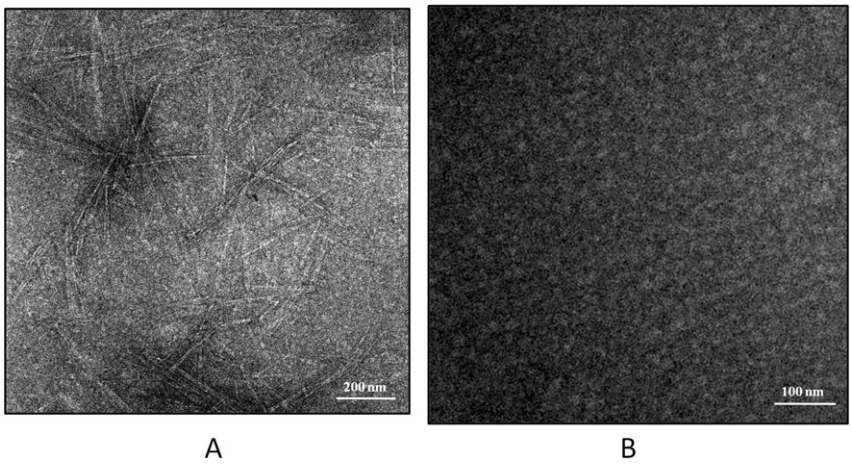

Fig. 6. Transmission electron microscopy. Human insulin incubated in the absence and in the presence of 0.5 M D-ribose and 5 mM methylglyoxal for 8 days was incubated with stirring at 37 °C for 24 h. The images are relative to D-ribose glycated insulin. Similar results were obtained for methylglyoxal glycated insulin.

for the non glycated insulin, being the protein in the harmless fibrillar form. On the contrary, the MTT reduction decreased significantly to 40% ($P < 0.001$) when the cells were exposed for 24 h to glycated insulin sample. These results could suggest that glycation of insulin inhibits fibril formation maintaining the protein in a pre-fibrillar, highly cytotoxic state. Alternatively, AGE adducts could be responsible per se for the cell toxicity. To better elucidate this aspect, we performed the MTT assay incubating the cells with glycated insulin before stirring, i.e., in condition in which the protein does not aggregate. Also in this case, the glycated protein appeared highly cytotoxic indicating that the toxicity is associated with the formation of the glycated adducts. Transmission electron microscopy measurements further confirmed this data (Fig. 6). Indeed, consistent with the ThT staining and the MTT assay, the TEM images recorded at 24 h from the onset of aggregation revealed

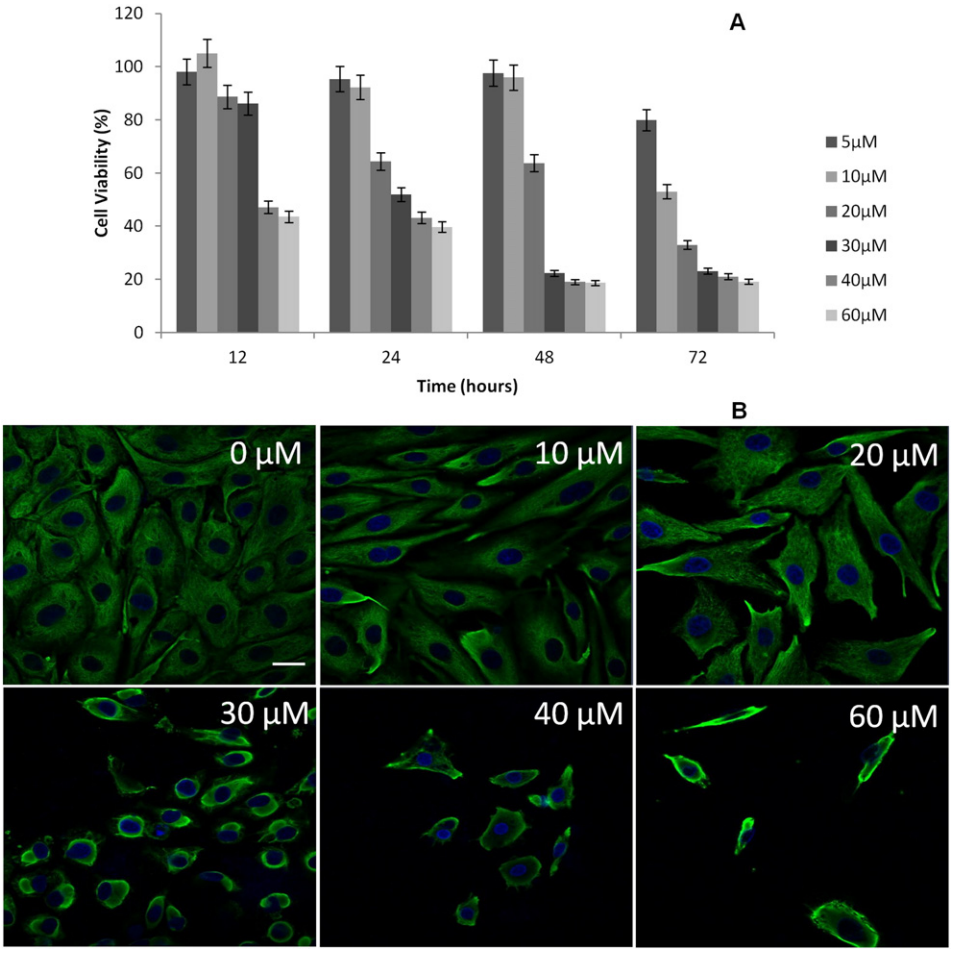

Fig. 7. Effect of ribose-glycated insulin on cell viability. EC were exposed for 12, 24, 48, and 72 h to increasing concentrations of glycated insulin (from 5 up to 60 μM) and cell viability was evaluated by MTT assay (panel A). Data are expressed as average percentage of MTT reduction ± SD relative to control cells from triplicate wells from 5 separate experiments ($P < 0.01$). EC morphology exposed to increasing concentration of ribose glycated insulin for 24 h (panel B). Scale bar represents 20 μm. EC treatment with non-glycated insulin did not show cell viability reduction.

the presence of mature fibrils only in the absence of glycating agent. No prefibrillar aggregates were detected in the sample glycated with D-ribose. Similar results were obtained in the presence of 5 mM methylglyoxal.

Taken together, our results indicate that glycation of the human insulin with both D-ribose and methylglyoxal strongly inhibits its ability to form amyloid aggregates.

3.4. Cytotoxicity of ribose-glycated insulin

The cytotoxicity of glycated insulin detected on NIH-3T3 cells encouraged us to investigate the mechanisms underlying the toxic effect. For this purpose, we focused our attention on endothelial cells (ECs), an appropriate cell model to investigate the endothelial dysfunction during diabetes and its vascular complications.

First, we evaluated the dose-dependent effect of ribose-glycated insulin on EC proliferative capacity. For this purpose, cells were exposed for 12, 24, 48, and 72 h to increasing concentrations of glycated insulin (from 5 up to 60 μM) (Fig. 7A). The results show that ribose-glycated insulin affects cell viability in a dose- and time-dependent manner. The EC proliferation index after treatment with lower concentrations of glycated insulin (5–10 μM) was significantly lower than that of the control cells at 72 h ($P < 0.05$, $P < 0.01$). Instead, at a concentration of 20 μM, the glycated insulin affected cell viability from 24 h of incubation ($P < 0.01$). Finally, EC viability resulted to be affected even after 12 h of incubation when concentrations of glycated insulin were 40, and 60 μM ($P < 0.01$).

As confirmed by EC morphological evaluation, ribose-glycated insulin is able to markedly induce cell cytoskeletal alteration (Fig. 7B). Indeed, as a result of the treatment with ribose-glycated insulin for 24 h, the ECs became spherical and this major morphological change was dose-dependent. In particular, at concentrations of 30, 40, and 60 μM the EC number was also consistently reduced. This evidence strongly supports the hypothesis that ribose-glycated insulin is highly cytotoxic. On the basis of these results, the 30 μM concentration of ribose-glycated insulin was chosen to further elucidate the mechanism by which glycated insulin induces cytotoxicity.

3.5. Effect of ribose-glycated insulin on cell cycle, apoptosis and ROS production

To study the effects on cell cycle distribution upon treatment with glycated insulin, FACS analyses were performed (Fig. 8). EC cells were treated with ribose-glycated insulin and a time course was carried out for 24, 48 and 72 h.

Cell cycle analysis (Fig. 8A, left panel) displayed that glycated insulin did not induce appreciable changes in cell cycle phases at 12 h of treatment (data not shown), but it was able to significantly alter cell cycle at 24 h of treatment. In particular, a strong reduction of cells in G1 phase together with an increase of S phase was detected. On the other hand, ribose-glycated insulin sensitized cells to death with an increase of Pre-G1 phase at 48 and 72 h of treatment (20,44% and 49,43%, respectively) (Fig. 8A, right panel). In order to discriminate the cell death pathways activated by the treatment, we monitored the enzymatic activity of the initiator caspases 8 and 9 and of the effector caspases 3/7 using flow cytometry. The results showed that after 72 h, glycated insulin significantly activated the initiator caspase 9 in the presence of inactive caspase 8, followed by activation of the effector caspases 3/7 (Fig. 8B). These data suggest an involvement of the mitochondrial pathways of apoptosis and a potential ROS activation. In line, to test whether

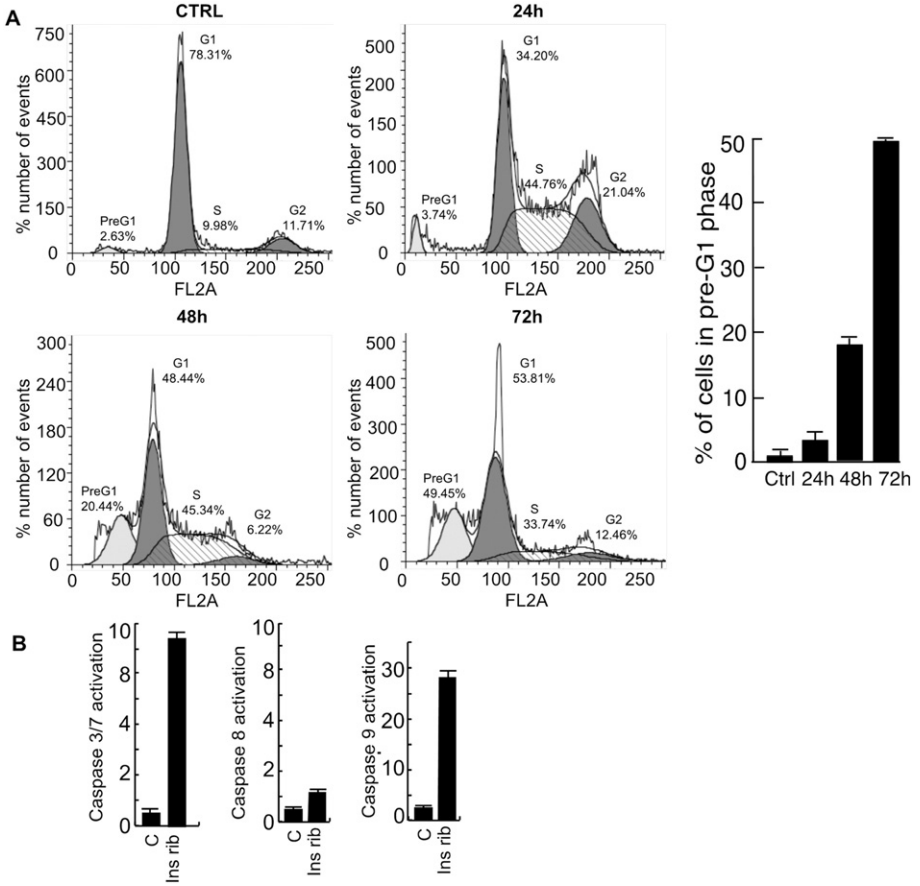

Fig. 8. Effect of ribose-glycated insulin on cell cycle and apoptosis. EC were treated with glycated insulin (30 μM) for 24, 48 and 72 h. Cell cycle (panel A, left) and pre-G1 evaluation (panel A, right) were evaluated by flow cytometric analysis. Caspase 3/7, caspase 8 and caspase 9 were evaluated by flow cytometric after 72 h of treatment (panel B). Cells untreated were used as control. Other experimental conditions are described in the Materials and methods section.

oxidative stress plays an important role in the death of ECs induced by glycated insulin, we measured the intracellular ROS level using the redox-sensitive fluorescent dye DCFH-DA. As shown in Fig. 9, cell exposure to ribose-glycated insulin for 24, 48 and 72 h led to a significant increase in intracellular ROS compared to control cells and cells treated with insulin alone after 72 h of exposure. Moreover, ECs were pretreated for 1 h with 20 mM N-acetylcysteine (NAC), a well-known ROS inhibitor. The presence of NAC was able to strongly inhibit the generation of intracellular ROS in cells exposed to glycated insulin to the same level of the untreated cells (Fig. 9). Clearly, glycated insulin promotes intracellular ROS production.

3.6. NF-kB activation by glycated insulin

Cellular effects induced by protein glycation have been reported to be mediated by specific AGE receptors (RAGE) [48,50,54,79]. In fact, glycation may be responsible, via RAGE, for an increase in oxidative stress and inflammation through the formation of ROS and the activation of the NF-kB [80]. In its inactive state, NF-kB is maintained as a latent form present in the cytoplasm where it is bound to a protein complex that masks the nuclear localization signal. In order to check the NF-kB involvement, we performed a confocal immunofluorescent assay on ECs incubated for 72 h with insulin and insulin glycated with D-ribose. The results are shown in Fig. 10 A and B. Exposure of cells to the ribose glycated insulin resulted in NF-kB activation, as depicted by its immunofluorescence signal. Moreover, the Western blot analysis shows a significant 14-fold increase in the amount of NF-κB/p65 in the nucleus (Fig. 10C).

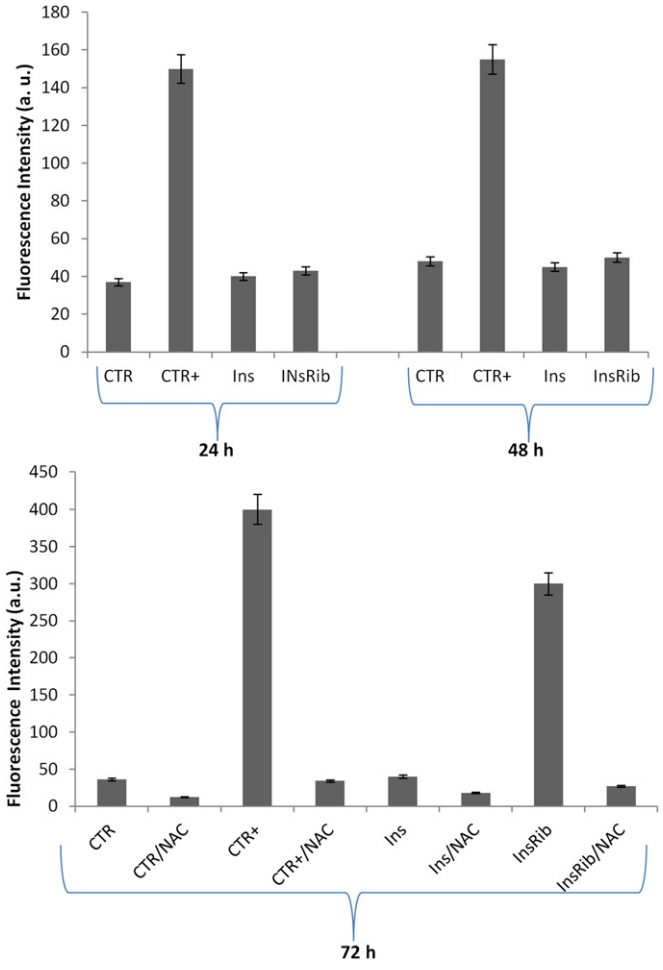

Fig. 9. Effect of ribose-glycated insulin on ROS production. Levels of ROS were determined by the DCFH-DA assay as described in Material and methods section. EC were exposed to insulin samples (30 μM) for 24, 48 and 72 h. ROS production was also tested in the presence of NAC at 72 h. CTR: untreated cells, CTR+: cells treated with 1.0 mM H_2O_2, Ins: cells treated with non-glycated insulin, InsRib: cells treated with ribose-glycated insulin. Other experimental conditions are described in the Materials and methods section.

4. Discussion

Insulin plays a central role in blood glucose homeostasis and is associated with a pathological condition termed insulin injection amyloidosis, characterized by the formation and deposition of amyloid fibrils. Insulin is a target of protein glycation because of its main physiological role. Glycation has been associated with human conformational diseases, such as Alzheimer's disease, transmissible spongiform encephalopathies, and familial amyloidosis, the hallmark of which is the presence of amyloid aggregates in the affected tissues. The majority of the cases are sporadic, suggesting that several factors must contribute to the onset and progression of these disorders. Recently, glycation of proteins has been reported to stimulate protein aggregation and amyloid deposition [35–43]. However, the effects induced by glycation may not be generalized since they are strongly dependent on the protein structure and glycating agent [41].

In this paper, we first examined the effects induced by insulin ribosylation on the structure and ability to form amyloid aggregates, comparing the results with those observed using methylglyoxal as glycating agent. Our data show that AGE modification of human insulin slightly affects the secondary structure content which, at the end of glycation reaction, i.e., after 7 days of incubation in the presence of 0.5 M D-ribose, consists in about 22% decrease of helical content and a corresponding increase of unordered structure. Furthermore, the AGE-insulin adduct does not show any predisposition to form AGE-cross-linked oligomers as proved by native and SDS-PAGE.

However, the most relevant observation is that D-ribose modification of insulin strongly inhibits amyloid fibril formation. In fact, incubation of glycated insulin under aggregating conditions produced lack of protein aggregation, no ThT binding and a CD spectrum similar to the one of the native protein. These results suggest that ribose-glycation of insulin inhibits the α-helix to β-sheet transition characteristic of the amyloid fibril formation maintaining the protein in a soluble form. Recently, Oliveira et al. [46] have analyzed the effects of methylglyoxal on the structure, stability and fibril formation of insulin. The Authors show that the modification of a single residue, i.e., Arg22 of the B-chain, reduces the ability of insulin to form amyloid fibrils by blocking the formation of seeding nuclei. They proposed that a higher dynamics in glycated insulin could lead to an impairment of the rigid cross-β structure formation and stabilize soluble aggregates in which each species retains a native-like structure. In our experiments, we did not observe both formation of aggregates and AGE-cross-linked oligomers. This could be caused by the different chemical modifications induced by D-ribose exposure. Alternatively, the differences may be explained by the experimental conditions used by Oliveira et al. [46]. In fact, in their study, glycation reaction and aggregation process simultaneously occur, thus triggering a drift from an amyloid aggregation to a native-like aggregation pathway [46]. However, our results fully corroborate their main conclusion that insulin glycation inhibits amyloid fibril formation. More recently, it has been reported that, using D-glucose as glycating agent under experimental conditions similar to those employed in our study, i.e., long-term incubation under non-reducing condition, the glycated insulin exhibits a very low propensity for oligomerization [58]. The same Authors reported that, in these conditions, amyloid-like species were not produced. However, it must be pointed out that insulin glycation by D-glucose modifies the N-terminus of both chains and the amino group of Lys B29 on the C-terminal region of chain B. Moreover, our observation that the extent of fluorescence quenching is largely different between D-ribose- and methylglyoxal-insulin adducts further corroborates that the two classes of glycating

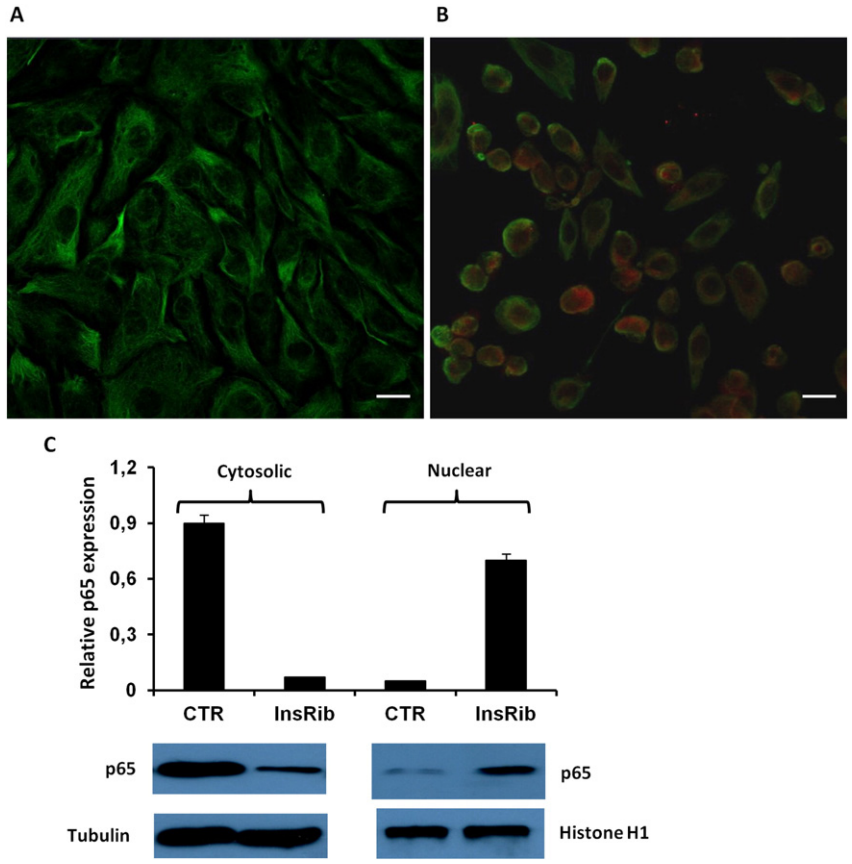

Fig. 10. Effect of ribose-glycated insulin on NF-kB activation. Representative confocal images of EC treated for 72 h with non-glycated (A) and glycated- (B) insulin (30 μM). Cells were incubated with specific antibodies against NF-kB/p65 (red) and Vimentin (green). Scale bar represents 20 μm. Western blot analysis of NF-kB/p65 expression for cytosolic and nuclear fractions (C). Other experimental conditions are described in the Materials and methods section.

agents, i.e., reducing sugars and methylglyoxal, react with different amino groups.

It is well established that the amyloid cytotoxicity is due to the first soluble oligomeric aggregates formed in the early stage of fibrillation process, whereas mature amyloid fibrils are essentially harmless. The inhibition of fibril formation upon ribose-glycation could indicate that glycation of insulin keep the protein in a pre-fibrillar, highly cytotoxic state. Our results showed that the ribose-glycated insulin was able to affect cell viability both before and after aggregating conditions, suggesting that the cytotoxicity is due to the AGEs insulin adducts. This finding was also confirmed by electron microscopy images showing absence of aggregate species in the glycated samples. In particular, the EC exposure to ribose-glycated insulin induced an alteration in cell cycle progression already at 24 h of treatment with a significant cellular death at 48 and 72 h as evaluated by cytofluorometry. This data was confirmed by the activation of initiator caspase 9 and effector caspase3/7 after 72 h of treatment. Moreover, we found that the exposure of EC to ribose-glycated insulin for 72 h generated intracellular ROS. This observation is in line with previous reports showing that ROS production increases in AGE-induced toxicity for several cell lines [81-84]. ROS have been identified as signaling molecules for signal transduction of several receptors, including the cell-associated receptor for AGEs, RAGE. An important issue dealing with the signaling cascade evoked by AGE treatment is the mechanism by which it causes oxidative stress. Previous studies indicate that AGE proteins prepared in vitro possess similar cross-reactive AGE epitopes that are common to proteins modified by AGEs in vivo and that interaction of these molecules with RAGE is associated with ROS generation and NF-kB activation [55,85-88]. The transcription factor NF-kB is a pleiotropic regulator of the inducible expression of many genes and it is activated by a wide variety of stimuli associated with stress and injury [89]. NF-kB is a dimer of two proteins (one of which is p65) localized in the cytoplasm of un-stimulated cells and it can be rapidly induced to enter the nucleus by appropriate signaling events, including ROS production, as observed in our study. Indeed, we found that NF-kB is activated in ECs after exposure to glycated insulin. Thus, the intracellular oxidative products and the subsequent activation of multiple signaling molecules, including NF-kB, could mediate the effects of ribose-glycated insulin in EC cells. Additional experiments are needed to evaluate the upstream signaling pathway and the involvement of the specific receptor RAGE.

5. Conclusions

In conclusion, the present study support the concept that the effects induced by glycation on amyloid aggregation may not be generalized as strongly depending on the protein structure. Indeed, being a post-translational modification, glycation can differently influence the aggregation process in promoting, accelerating and/or stabilizing on-pathway and off-pathway species. Indeed, insulin glycation with D-ribose prevents the amyloid fibril formation keeping the protein in a soluble state. Moreover, the AGE-modified insulin when incubated with endothelial cells induces cell dysfunction initiated by ROS production and NF-kB activation. As observed for other glycated proteins, this effect could be likely mediated by the interaction of AGE-modified protein with RAGE. Since accumulation of AGEs has been suggested as one of the main responsible factors of diabetes-associated complications, such as retinopathy, nephropathy, atherosclerosis, further examination of the molecular bases underlying the toxic effect produced by AGE-modified insulin on neighboring cells may help to identify new therapeutic interventions.

Acknowledgments

This work was supported by a grant from "Regione Campania (L.R. N.5-28.03.2002"; EU: the Blueprint High Impact Project and MIUR (PRIN 2012ZHN9YH). The authors wish to thank the "Electron Microscopy" Facility of the Department of Experimental Medicine—"Laboratorio Grandi Attrezzature"—Second University of Naples, and Marcella Cammarota for her skilled technical support.

References

[1] M.J. Adams, T.L. Blundell, E.J. Dodson, G.G. Dodson, M. Vijayan, E.N. Baker, M.M. Harding, D.C. Hodgkin, B. Rimmer, S. Sheat, Structure of rhombohedral 2 zinc insulin crystal, Nature 224 (1969) 491–495.
[2] G. Dodson, D. Steiner, The role of assembly in insulin's biosynthesis, Curr. Opin. Struct. Biol. 8 (2) (1998) 189–194.
[3] M.F. Dunn, Zinc-ligand interactions modulate assembly and stability of the insulin hexamer — a review, Biometals 18 (4) (2005) 295–303.
[4] F. Chiti, C.M. Dobson, Protein misfolding, functional amyloid, and human disease, Annu. Rev. Biochem. 75 (2006) 333–366.
[5] F.E. Dische, C. Wernstedt, G.T. Westermark, P. Westermark, M.B. Pepys, J.A. Rennie, S.G. Gilbey, P.J. Watkins, Insulin as an amyloid-fibril protein at sites of repeated insulin injections in a diabetic patient, Diabetologia 31 (3) (1988) 158–161.
[6] P. Westermark, M.D. Benson, J.N. Buxbaum, A.S. Cohen, B. Frangione, S. Ikeda, C.L. Masters, G. Merlini, M.J. Saraiva, J.D. Sipe, Nomenclature Committee of the International Society of Amyloidosis. Amyloid: Toward terminology clarification report from the nomenclature committee of the international society of amyloidosis. Amyloid 12 (1) (2005) 1–4.
[7] S. Okamura, Y. Hayashino, S. Kore-Eda, S. Tsujii, Localized amyloidosis at the site of repeated insulin injection in a patient with type 2 diabetes, Diabetes Care 36 (12) (2013), e200http://dx.doi.org/10.2337/dc13-1651.
[8] T. Nagase, K. Iwaya, Y. Iwaki, F. Kotake, R. Uchida, T. Oh-i, H. Sekine, K. Miwa, S. Murakami, T. Odaka, M. Kure, Y. Nemoto, M. Noritake, Y. Katsura, Insulin-derived amyloidosis and poor glycemic control: a case series, Am. J. Med. 127 (5) (2014) 450–454, http://dx.doi.org/10.1016/j.amjmed.2013.10.029.
[9] A. D'Souza, J.D. Theis, J.A. Vrana, A. Dogan, Pharmaceutical amyloidosis associated with subcutaneous insulin and enfuvirtide administration, Amyloid 21 (2) (2014) 71–75, http://dx.doi.org/10.3109/13506129.2013.876984.
[10] E. Herczenik, M.F. Gebbink, Molecular and cellular aspects of protein misfolding and disease, FASEB J. 22 (7) (2008) 2115–2133, http://dx.doi.org/10.1096/fj.07-099671.
[11] A. Ahmad, V. Uversky, D. Hong, A. Fink, Early events in the fibrillation of monomeric insulin, J. Biol. Chem. 280 (2005) 42669–42675.
[12] V. Foderà, S. Cataldo, F. Librizzi, B. Pignataro, P. Spiccia, M. Leone, Self-organization pathways and spatial heterogeneity in insulin amyloid fibril formation, J. Phys. Chem. B 113 (31) (2009) 10830–10837, http://dx.doi.org/10.1021/jp810972y.
[13] E.J. Nettleton, P. Tito, M. Sunde, M. Bouchard, C.M. Dobson, C.V. Robinson, Characterization of the oligomeric states of insulin in self-assembly and amyloid fibril formation by mass spectrometry, Biophys. J. 79 (2) (2000) 1053–1065.
[14] M. Bouchard, J. Zurdo, E.J. Nettleton, C.M. Dobson, C.V. Robinson, Formation of insulin amyloid fibrils followed by FTIR simultaneously with CD and electron microscopy, Protein Sci. 9 (10) (2000) 1960–1967.
[15] B. Vestergaard, M. Groenning, M. Roessle, J.S. Kastrup, M. van de Weert, J.M. Flink, S. Frokjaer, M. Gajhede, D.I. Svergun, A helical structural nucleus is the primary elongating unit of insulin amyloid fibrils, PLoS Biol. 5 (5) (2007), e134.
[16] J. Brange, L. Andersen, E.D. Laursen, G. Meyn, E. Rasmussen, Toward understanding insulin fibrillation, J. Pharm. Sci. 86 (1997) 517–525, http://dx.doi.org/10.1021/js960297s.
[17] Y.H. Abdel-Wahab, F.P. O'Harte, H. Ratcliff, N.H. McClenaghan, C.R. Barnett, P.R. Flatt, Glycation of insulin in the islets of Langerhans of normal and diabetic animals, Diabetes 45 (11) (1996) 1489–1496.
[18] Y.H. Abdel-Wahab, F.P. O'Harte, A. Boyd, C. Barnett, P. Flatt, Glycation of insulin results in reduced biological activity in mice, Acta Diabetol. 34 (1997) 265–270.
[19] A.C. Boyd, Y.H. Abdel-Wahab, A.M. McKillop, H. McNulty, C.R. Barnett, F.P. O'Harte, P.R. Flatt, Impaired ability of glycated insulin to regulate plasma glucose and stimulate glucose transport and metabolism in mouse abdominal muscle, Biochim. Biophys. Acta 1523 (1) (2000) 128–134.
[20] R. Singh, A. Barden, T. Mori, N. Beilin, Advanced glycation end-products: a review, Diabetologia 44 (2001) 129–146.
[21] P. Ulrich, A. Cerami, Protein glycation, diabetes, and aging, Recent Prog. Horm. Res. 56 (2001) 1–21.
[22] M. Lu, M. Kuroki, S. Amano, M. Tolentino, K. Keough, I. Kim, R. Bucala, A.P. Adamis, Advanced glycation end products increase retinal vascular endothelial growth factor expression, J. Clin. Invest. 101 (1998) 1219–1224.
[23] M. Brownlee, Negative consequences of glycation, Metabolism 49 (2000) 9–13.
[24] E. Schleicher, U. Friess, Oxidative stress, AGE, and atherosclerosis, Kidney Int. Suppl. 106 (2007) S17–S26.
[25] K. Fukami, S. Yamagishi, S. Ueda, S. Okuda, Role of AGEs in diabetic nephropathy, Curr. Pharm. Des. 14 (10) (2008) 946–952.
[26] S.F. Yan, R. Ramasamy, A.M. Schmidt, Receptor for AGE (RAGE) and its ligands cast into leading roles in diabetes and the inflammatory response, J. Mol. Med. 87 (2009) 235–247, http://dx.doi.org/10.1007/s00109-009-0439-2.
[27] A. Bierhaus, P.P. Nawroth, Multiple levels of regulation determine the role of the receptor for AGE (RAGE) as common soil in inflammation, immune responses and diabetes mellitus and its complications, Diabetologia 52 (11) (2009) 2251–2263, http://dx.doi.org/10.1007/s00125-009-1458-9.
[28] A.W. Stitt, AGEs and diabetic retinopathy, Invest. Ophthalmol. Vis. Sci. 51 (10) (2010) 4867–4874, http://dx.doi.org/10.1167/iovs.10-5881.
[29] V. Miranda, T.F. Outeiro, The sour side of neurodegenerative disorders: the effects of protein glycation, J. Pathol. 221 (1) (2010) 13–25, http://dx.doi.org/10.1002/path.2682.
[30] J. Li, D. Liu, L. Sun, Y. Lu, Z. Zhang, Advanced glycation end products and neurodegenerative diseases: mechanisms and perspective, J. Neurol. Sci. 317 (1–2) (2012) 1–5, http://dx.doi.org/10.1016/j.jns.2012.02.018.
[31] M.A. Smith, S. Taneda, P.L. Richey, S. Miyata, S.D. Yan, D. Stern, L.M. Sayre, V.M. Monnier, G. Perry, Advanced Maillard reaction end products are associated with Alzheimer disease pathology, Proc. Natl. Acad. Sci. U. S. A. 91 (1994) 5710–5714.
[32] M.P. Vitek, K. Bhattacharya, J.M. Glendening, E. Stopa, H. Vlassara, R. Bucala, K. Manogue, A. Cerami, Advanced glycation end products contribute to amyloidosis in Alzheimer disease, Proc. Natl. Acad. Sci. U. S. A. 91 (11) (1994) 4766–4770.
[33] S.D. Yan, X. Chen, A.M. Schmidt, J. Brett, G. Godman, Y.S. Zou, C.W. Scott, C. Caputo, T. Frappier, M.A. Smith, G. Perry, S.H. Yen, D. Stern, Glycated tau protein in Alzheimer disease: a mechanism for induction of oxidant stress, Proc. Natl. Acad. Sci. U. S. A. 91 (1994) 7787–7791.
[34] R. Gomes, M. Sousa Silva, A. Quintas, C. Cordeiro, A. Freire, P. Pereira, A. Martins, E. Monteiro, E. Barroso, A. Ponces Freire, Argpyrimidine, a methylglyoxal-derived advanced glycation end-product in familial amyloidotic polyneuropathy, Biochem. J. 385 (2005) 339–345.
[35] G. Munch, S. Mayer, J. Michaelis, A.R. Hipkiss, P. Riederer, R. Müller, A. Neumann, R. Schinzel, A.M. Cunningham, Influence of advanced glycation end-products and AGE-inhibitors on nucleation-dependent polymerization of beta-amyloid peptide, Biochim. Biophys. Acta 1360 (1997) 17–29, http://dx.doi.org/10.1016/S0925-4439(96)00062-2.
[36] G. Munch, H.J. Luth, A. Wong, T. Arendt, E. Hirsch, R. Ravid, P. Riederer, Crosslinking of alpha-synuclein by advanced glycation endproducts-an early pathophysiological step in Lewy body formation? J. Chem. Neuroanat. 20 (2000) 253–257, http://dx.doi.org/10.1016/S0891-0618(00)00096-X.
[37] C. Loske, A. Gerdemann, W. Schepl, M. Wycislo, R. Schinzel, D. Palm, P. Riederer, G. Münch, Transition metal-mediated glycoxidation accelerates cross-linking of β-amyloid peptide, Eur. J. Biochem. 267 (2001) 4171–4178.
[38] B. Bouma, L.M. Kroon-Batenburg, Y.P. Wu, B. Brunjes, G. Posthuma, O. Kranenburg, P.G. de Groot, E.E. Voest, M.F. Gebbink, Glycation induces formation of amyloid cross-beta structure in albumin, J. Biol. Chem. 278 (2003) 41810–41819, http://dx.doi.org/10.1074/jbc.M303925200.
[39] F.L. Kong, W. Cheng, J. Chen, Y. Liang, D-ribose glycates b2-microglobulin to form aggregates with high cytotoxicity through a ROS-mediated pathway, Chem. Biol. Interact. 194 (2011) 69–78, http://dx.doi.org/10.1016/j.cbi.2011.08.003.
[40] T.A. Khan, S. Amani, A. Naeem, Glycation promotes the formation of genotoxic aggregates in glucose oxidase, Amino Acids 43 (2012) 1311–1322, http://dx.doi.org/10.1007/s00726-011-1204-8.
[41] C. Iannuzzi, G. Irace, I. Sirangelo, Differential effects of glycation on protein aggregation and amyloid formation, Front. Mol. Biosci. 1 (2014) 9, http://dx.doi.org/10.3389/fmolb.2014.00009.
[42] L. Chen, Y. Wei, X.Q. Wang, R.Q. He, Ribosylation rapidly induces alpha-synuclein to form highly cytotoxic molten globules of advanced glycation end products, PLoS One 5 (2010), e9052http://dx.doi.org/10.1371/journal.pone.0009052.
[43] L. Chen, Y. Wei, X.Q. Wang, R.Q. He, D-ribosylated tau forms globular aggregates with high cytotoxicity, Cell. Mol. Life Sci. 66 (2009) 2559–2571, http://dx.doi.org/10.1007/s00018-009-0058-7.
[44] N. Hashimoto, H. Naiki, F. Gejyo, Modification of beta 2-microglobulin with D-glucose or 3-deoxyglucosone inhibits A beta 2 M amyloid fibril extension in vitro, Amyloid 6 (1999) 256–264.
[45] D. Lee, C.W. Park, S.R. Paik, K.Y. Choi, The modification of α-synuclein by dicarbonyl compounds inhibits its fibril-forming process, Biochim. Biophys. Acta 1794 (2009) 421–430, http://dx.doi.org/10.1016/j.bbapap.2008.11.016.
[46] L.M. Oliveira, A. Lages, R.A. Gomes, H. Neves, C. Família, A.V. Coelho, A. Quintas, Insulin glycation by methylglyoxal results in native-like aggregation and inhibition of fibril formation, BMC Biochem. 12 (2011) 41, http://dx.doi.org/10.1186/1471-2091-12-41.
[47] C. Iannuzzi, V. Carafa, L. Altucci, G. Irace, M. Borriello, R. Vinciguerra, I. Sirangelo, Glycation of wild-type apomyoglobin induces formation of highly cytotoxic species. J. Cell. Physiol. (2015)http://dx.doi.org/10.1002/jcp.25011.
[48] D.M. Stern, S.D. Yan, S.F. Yan, A.M. Schmidt, Receptor for advanced glycation endproducts (RAGE) and the complications of diabetes, Ageing Res. Rev. 1 (2002) 1–15.
[49] M. Peppa, J. Uribarri, H. Vlassara, Glucose, advanced glycation end products, and diabetes complications: what is new and what works, Clin. Diab. 21 (2003) 186–187.
[50] A. Goldin, J.A. Beckman, A.M. Schmidt, M.A. Creager, Advanced glycation end products: sparking the development of diabetic vascular injury, Circulation 114 (2006) 597–605, http://dx.doi.org/10.1161/CIRCULATIONAHA.106.621854.
[51] T. Su, R.Q. He, D-ribose, an overlooked player in type 2 diabetes mellitus? Sci. China Life Sci. 57 (2014) 361, http://dx.doi.org/10.1007/s11427-014-4614-5.
[52] K. Kierdorf, G. Fritz, RAGE regulation and signaling in inflammation and beyond, J. Leukoc. Biol. 94 (1) (2013) 55–68, http://dx.doi.org/10.1189/jlb.1012519.
[53] N. Nass, B. Bartling, A. Navarrete Santos, R.J. Scheubel, J. Börgermann, R.E. Silber, A. Simm, Advanced glycation end products, diabetes and ageing, Z. Gerontol. Geriatr. 40 (5) (2007) 349–356.

[54] C. Ott, K. Jacobs, E. Haucke, A.N. Santos, N. Grune, A. Simm, Role of advanced glycation end products in cellular signaling, Redox Biol. 2 (2014) 411–429, http://dx.doi.org/10.1016/j.redox.2013.12.016.
[55] C.S. Han, Y. Lu, Y. Wei, B. Wu, Y. Liu, R.Q. He, D-ribosylation induces cognitive impairment through RAGE-dependent astrocytic inflammation, Cell Death Dis. 5 (2014), e1117http://dx.doi.org/10.1038/cddis.2014.89.
[56] F.P.M. O'Harte, P. Højrup, C.R. Barnett, P.R. Flatt, Identification of the site of glycation of human insulin, Peptides 17 (1996) 1323–1330.
[57] S. Guedes, R. Vitorino, M.R. Domingues, F. Amado, P. Domingues, Mass spectrometry characterization of the glycation sites of bovine insulin by tandem mass spectrometry, J. Am. Soc. Mass Spectrom. 20 (2009) 1319–1326, http://dx.doi.org/10.1016/j.jasms.2009.03.004.
[58] P. Alavi, R. Yousefi, S. Amirghofran, H.R. Karbalaei-Heidari, A.A. Moosavi-Movahedi, Structural analysis and aggregation propensity of reduced and nonreduced glycated insulin adducts, Appl. Biochem. Biotechnol. 170 (2013) 623–638, http://dx.doi.org/10.1016/j.ijbiomac.2012.05.021.
[59] Y. Wei, L. Chen, J. Chen, L. Ge, R.Q. He, Rapid glycation with D-ribose induces globular amyloid-like aggregations of BSA with high cytotoxicity to SH-SY5Y cells, BMC Cell. Biol. 10 (2009) 10, http://dx.doi.org/10.1186/1471-2121-10-10.
[60] T. Su, L. Xin, Y.G. He, Y. Wei, Y.X. Song, W.W. Li, X.M. Wang, R.Q. He, The abnormally high level of uric D-ribose for type-2 diabetics, Prog. Biochem. Biophys. 40 (9) (2013) 816–825.
[61] T. Oya, N. Hattori, Y. Mizuno, S. Miyata, S. Maeda, T. Osawa, K. Uchida, Methylglyoxal modification of protein. Chemical and immunochemical characterization of methylglyoxal-arginine adducts. J. Biol. Chem. 274 (1999) 18492–18502.
[62] N. Sreerama, R.W. Woody, Estimation of protein secondary structure from circular dichroism spectra: comparison of CONTIN, SELCON, and CDSSTR methods with an expanded reference set, Anal. Biochem. 287 (2000) 252–260.
[63] M.B. Hansen, S.E. Nielsen, K. Berg, Re-examination and further development of a precise and rapid dye method for measuring cell growth/cell kill, J. Immunol. Methods 119 (1989) 203–210.
[64] I. Sirangelo, C. Iannuzzi, S. Vilasi, G. Irace, G. Giuberti, G. Misso, A. D'Alessandro, A. Abbruzzese, M. Caraglia, W7FW14F apomyoglobin amyloid aggregates-mediated apoptosis is due to oxidative stress and AKT inactivation caused by ras and Rac, J. Cell. Physiol. 221 (2009) 412–423, http://dx.doi.org/10.1002/jcp.21871.
[65] A. Nebbioso, N. Clarke, E. Voltz, E. Germain, C. Ambrosino, P. Bontempo, R. Alvarez, E.M. Schiavone, F. Ferrara, F. Bresciani, A. Weisz, A.R. de Lera, H. Gronemeyer, L. Altucci, Tumor-selective action of HDAC inhibitors involves TRAIL induction in acute myeloid leukemia cells, Nat. Med. 11 (2005) 77–84.
[66] A. Nebbioso, F. Manzo, M. Miceli, M. Conte, L. Manente, A. Baldi, A. De Luca, D. Rotili, S. Valente, A. Mai, A. Usiello, H. Gronemeyer, L. Altucci, Selective class II HDAC inhibitors impair myogenesis by modulating the stability and activity of HDAC-MEF2 complexes, EMBO Rep. 10 (2009) 776–782, http://dx.doi.org/10.1038/embor.2009.88.
[67] L. Servillo, N. D'Onofrio, L. Longobardi, I. Sirangelo, A. Giovane, D. Cautela, D. Castaldo, A. Giordano, M.L. Balestrieri, Stachydrine ameliorates high-glucose induced endothelial cell senescence and SIRT1 downregulation, J. Cell. Biochem. 114 (11) (2013) 2522–2530, http://dx.doi.org/10.1002/jcb.24598.
[68] S.B. Matiacevich, M.P. Buera, A critical evaluation of fluorescence as a potential marker for the maillard reaction, Food Chem. 95 (2006) 423–430.
[69] M. Adrover, L. Mariño, P. Sanchis, K. Pauwels, Y. Kraan, P. Lebrun, B. Vilanova, F. Muñoz, K. Broersen, J. Donoso, Mechanistic insights in glycation-induced protein aggregation, Biomacromolecules 15 (9) (2014) 3449–3462, http://dx.doi.org/10.1021/bm501077j.
[70] F. Morgan, J. Léonil, D. Mollé, S. Bouhallab, Modification of bovine β-lactoglobulin by glycation in a powdered state or in an aqueous solution: effect on association behavior and protein conformation, J. Agric. Food Chem. 47 (1999) 83–91.
[71] J.L. Wautier, P.J. Guillausseau, Advanced glycation and products, their receptors and diabetic angiopathy, Diabete Metab. 27 (2001) 535–542.
[72] C.C. Lee, A. Nayak, A. Sethuraman, G. Belfort, G.J. McRae, A three-stage kinetic model of amyloid fibrillation, Biophys. J. 92 (2007) 3448–3458.
[73] J.L. Jimenez, E.J. Nettleton, M. Bouchard, C.V. Robinson, C.M. Dobson, H.R. Saibil, The protofilament structure of insulin amyloid fibrils, Proc. Natl. Acad. Sci. U. S. A. 99 (2002) 9196–9201.
[74] M.I. Smith, J.S. Sharp, C.J. Roberts, Insulin fibril nucleation: the role of prefibrillar aggregates, Biophys. J. 95 (2008) 3400–3406, http://dx.doi.org/10.1529/biophysj.108.131482.
[75] M. Stefani, Structural features and cytotoxicity of amyloid oligomers: implication in Alzheimer's disease and other diseases with amyloid deposits, Prog. Neurobiol. 99 (2012) 226–245, http://dx.doi.org/10.1016/j.pneurobio.2012.03.002.
[76] S. Vilasi, C. Iannuzzi, M. Portaccio, G. Irace, I. Sirangelo, Effect of trehalose on W7FW14F apomyoglobin and insulin fibrillization: new insight into inhibition activity. Biochemistry 47 (6) (2008) 1789–1796, http://dx.doi.org/10.1021/bi701530w.
[77] S. Vilasi, R. Sarcina, R. Maritato, A. De Simone, G. Irace, I. Sirangelo, Heparin induces harmless fibril formation in amyloidogenic W7FW14F apomyoglobin and amyloid aggregation in wild-type protein in vitro, PLoS One 6 (2011), e22076http://dx.doi.org/10.1371/journal.pone.0022076.
[78] H.I.I.I. Levine, Thioflavine T interaction with synthetic Alzheimer's disease beta-amyloid peptides: setection of amyloid aggregation in solution, Protein Sci. 2 (1993) 404–410.
[79] N. Ohgami, R. Nagai, M. Ikemoto, H. Arai, A. Miyazaki, et al., CD36 serves as a receptor for advanced glycation end products (AGE), J. Diabet. Complicat. 16 (2002) 56–59, http://dx.doi.org/10.1016/S1056-8727(01)00208-2.
[80] J. Xie, J.D. Méndez, V. Méndez-Valenzuela, M.M. Aguilar-Hernández, Cellular signaling of the receptor for advanced glycation end products (RAGE), Cell. Signal. 25 (2013) 2185–2197, http://dx.doi.org/10.1016/j.cellsig.2013.06.013.
[81] S. Yamagishi, M. Takeuchi, Nifedipine inhibits gene expression of receptor for advanced glycation end products (RAGE) in endothelial cells by suppressing reactive oxygen species generation, Drugs Exp. Clin. Res. 30 (4) (2004) 169–175.
[82] M.A. Lal, H. Brismar, A.E. Ekof, A. Aperia, Role of oxidative stress in advanced glycation end product-induced mesangial cell activation, Kidney Int. 61 (6) (2002) 2006–2014.
[83] V. Scivittaro, M.B. Ganz, M.F. Weiss, AGEs induce oxidative stress and activate protein kinase C-beta(II) in neonatal mesangial cells, Am. J. Physiol. Ren. Physiol. 278 (4) (2000) F676.
[84] C.S. Han, Y. Lu, Y. Wei, Y. Liu, R.Q. He, D-ribose induces cellular protein glycation and impairs mouse spatial cognition, PLoS One 6 (2011), e24623http://dx.doi.org/10.1371/journal.pone.0024623.
[85] T. Kislinger, C. Fu, B. Huber, W. Qu, A. Taguchi, S.D. Yan, M. Hofmann, S.F. Yan, M. Pischetsrieder, D. Stern, A.M. Schmidt, N(epsilon)-(carboxymethyl)lysine adducts of proteins are ligands for receptor for advanced glycation end products that activate cell signaling pathways and modulate gene expression, J. Biol. Chem. 274 (44) (1999) 31740–31749.
[86] H.J. Huttunem, C. Fages, H. Rauvala, Receptor for advanced glycation and products (RAGE)-mediated neurite outgrowth and activation of NF-kappaB require the cytoplasmatic domain of the receptor but different downstream signaling pathways, J. Biol. Chem. 274 (1999) 19919–19924.
[87] L. Gu, S. Hagiwara, Q. Fan, M. Tanimoto, M. Kobata, M. Yamashita, T. Nishitani, T. Gohda, Z. Ni, J. Qian, S. Horikoshi, Y. Tomino, Role of receptor for advanced glycation end-products and signalling events in advanced glycation end-product-induced monocyte chemoattractant protein-1 expression in differentiated mouse podocytes, Nephrol. Dial. Transplant. 21 (2) (2006) 299–313.
[88] A.L. Wang, A.C. Yu, Q.H. He, X. Zhu, M.O. Tso, AGEs mediated expression and secretion of TNF alpha in rat retinal microglia, Exp. Eye Res. 84 (5) (2007) 905–913.
[89] N. Li, M. Karin, Is NF-kappaB the sensor of oxidative stress? FASEB J. 13 (10) (1999) 1137–1143.